cis-β Ruthenium Complexes with Sterically Bulky Salen Ligands. Enantioselective Intermolecular Carbene Insertion into Si–H Bonds and X-ray Crystal Structure of *cis-β*-[Ru^{II}(salen)(CO)(CPh_2)] Complex

Chi Lun Lee,[†,§] Daqing Chen,[†,‡,§] Xiao-Yong Chang,[†] Zhou Tang,[†] and Chi-Ming Che*[,†,ǁ]

[†] State Key Laboratory of Synthetic Chemistry and Department of Chemistry, The University of Hong Kong, Pokfulam Road, Hong Kong, P. R. China

[‡] School of Environment and Ecology, Jiangsu Open University, Nanjing 210000, P. R. China

[ǁ] HKU Shenzhen Institute of Research and Innovation, Shenzhen 518057, P. R. China

ABSTRACT: The synthesis, spectroscopy, crystal structure, and electrochemical behavior of *cis-β*-$Ru^{II}(CO)_2$, *cis-β*-$Ru^{II}(CO)(H_2O)$, and *cis-β*-Ru^{II}(CO)(carbene) complexes supported by sterically bulky salen ligands are described, along with catalytic activity of chiral *cis-β*-[Ru^{II}(salen)$(CO)_2$] complexes towards enantioselective carbene Si–H insertion using $N_2C(Ar)CO_2R$ as carbene source under light irradiation with product yields up to 96% and ee up to 84%. The *cis-β*-$Ru^{II}(CO)(H_2O)$ complex was isolated by using a binaphthyl salen ligand bearing bulky CPh_3 substituents, with the H_2O molecule coordinated at the site *trans* to an N_{imine} atom of the salen ligand. Light irradiation of a *cis-β*-$Ru^{II}(CO)_2$ complex, supported by a binaphthyl salen ligand with ^{t}Bu substituents, followed by treatment with N_2CAr_2 (Ar = Ph, *p*-ClC_6H_4) gave *cis-β*-[Ru^{II}(salen)(CO)(CAr_2)] which features a coordinated carbene ligand *trans* to a salen N_{imine} atom and undergoes carbene transfer to nitrosobenzene to give the corresponding nitrone product. These findings and related HR-ESI-MS studies provide evidence for the involvement of salen-supported *cis-β*-Ru^{II}(CO)(C(Ar)CO_2R) active species in the intermolecular carbene Si–H insertion reaction catalyzed by *cis-β*-[Ru^{II}(salen)$(CO)_2$] complexes.

INTRODUCTION

Chiral ruthenium-salen complexes offer versatile catalysts for various asymmetric organic transformation reactions,[1] including atom/group transfer reactions such as epoxidation,[1a,c,h,i] cyclopropanation,[1a,c,d,f-i] and aziridination[1h,i] of alkenes catalyzed by various Ru-salen complexes which bear tetradentate salen ligands adopting planar N_2O_2 arrangement as in *trans*-octahedral metal-salen complexes (Figure 1). In contrast, the synthesis and catalytic studies of Ru-salen complexes bearing non-planar N_2O_2 salen ligands, i.e. adopting a *cis* (*cis-α* or *cis-β*) configuration of octahedral metal-salen complexes[1d,g,i] (Figure 1, inset), are scarce.[1d,g] Different from *trans* metal-salen complexes, *cis* metal-salen complexes have two unique characteristics: (i) the metal atom is stereogenic, which promises an effective chirality transfer for organic reactions due to close proximity of the metal to the substrate in the inner coordination sphere; (ii) there are two mutually *cis* coordination sites which allow substrate binding and activation via an η^2 or η^1 coordination mode. In 2001, Scott and co-workers reported that a *cis-β*-[Ru^{II}(salen)$(MeCN)_2$] complex (inset of Figure 2) is an active catalyst for intermolecular alkene cyclopropanation with high diastereoselectivity and enantioselectivity via a proposed *cis-β*-Ru-salen carbene active intermediate (species **I** in the inset of Figure 2);[2] this *cis-β* species **I** has not been directly detected experimentally, in contrast to the isolation and X-ray crystal structural determination of several *trans*-

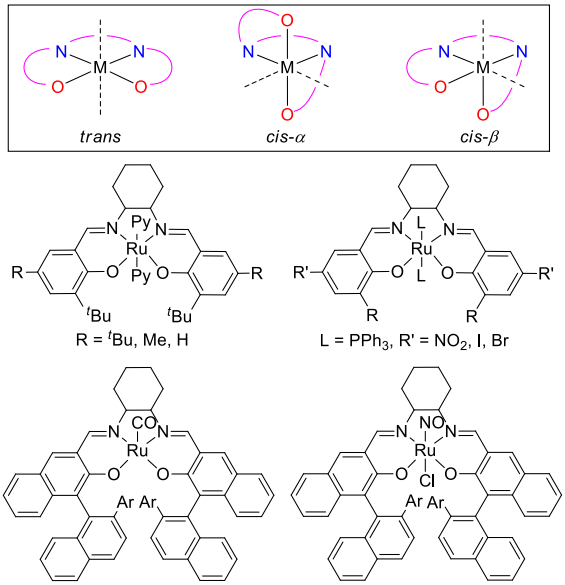

Figure 1. Literature reported examples of Ru-salen catalysts featuring planar N_2O_2 salen ligands. Inset: three possible configurations (*trans*, *cis-α*, and *cis-β*) of octahedral metal-salen complexes.

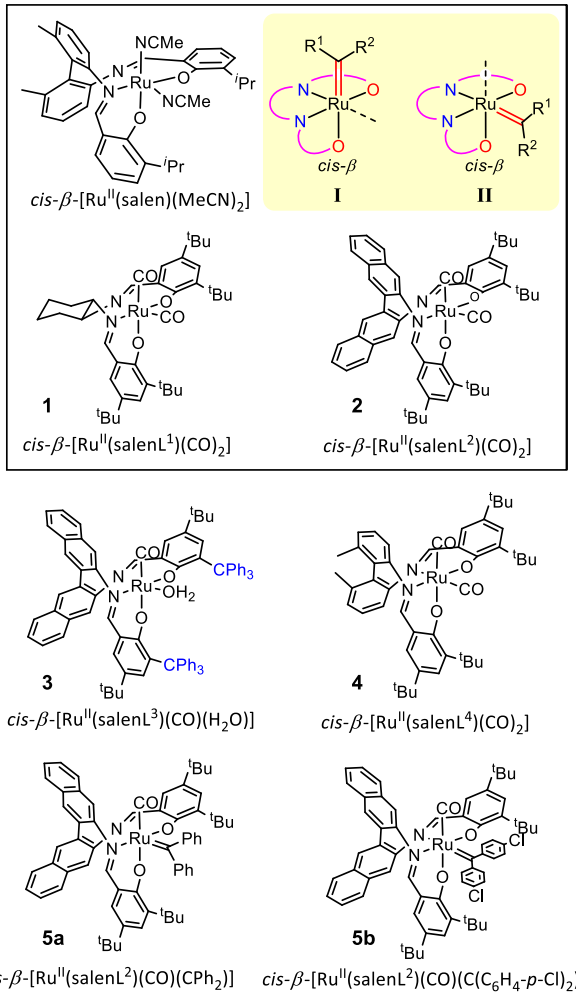

Figure 2. Examples of *cis-β* ruthenium-salen complexes. The previously reported ones,[2,5] together with proposed *cis-β* Ru-salen carbene intermediates, are depicted in the inset. Complexes **3**–**5** were first synthesized in this work.

Ru-salen carbene complexes.[3] Subsequently, Katsuki and coworkers reported asymmetric sulfimidation catalyzed by *cis-β*-[Ru^{II}(salalen)$(CO)_2$] complexes (salalen ligand resembles salen ligand except that one of the two imine groups in the latter becomes an amine group in the former);[4] we reported asymmetric intramolecular alkene cyclopropanation catalyzed by *cis-β*-[Ru^{II}(salen)$(CO)_2$] (e.g., *cis-β*-[Ru^{II}(salenL^1)$(CO)_2$] (**1**) and *cis-β*-[Ru^{II}(salenL^2)$(CO)_2$] (**2**) shown in the inset of Figure 2) under light irradiation which exhibits high enantioselectivity and possibly involves proposed elusive *cis-β*-Ru-salen carbene active intermediates **I** and/or **II** (inset of Figure 2).[5]

To obtain an isolable or directly detectable example of *cis-β*-Ru-salen carbene species and also explore new carbene transfer reactions catalyzed by *cis-β*-Ru-salen complexes, we directed our attention to sterically bulky salen ligands and carbene insertion into Si–H bonds giving silyl compounds. Construction of the compounds possessing silyl group(s) has received considerable attention.[6] Previously reported metal-catalyzed enantioselective carbene Si–H insertion reactions mostly employ, for example, chiral Cu(I), Rh(II), and Ir(III) catalysts;[7-13] for Ru-catalyzed carbene Si–H insertion, there is only one report,[14] which uses arylsilane substrates and a chiral Ru(II)-pheox catalyst (pheox: a bidentate cyclometalating phenyloxazoline C^N ligand), in contrast to a considerable number of reports on Ru-catalyzed other types of carbene transfer reactions particularly cyclopropanation of alkenes.[15-21]

Herein we report the synthesis and characterization of new chiral *cis-β*-Ru-salen complexes *cis-β*-[Ru^{II}(salenL^3)(CO)(H_2O)] (**3**) and *cis-β*-[Ru^{II}(salenL^4)$(CO)_2$] (**4**) bearing sterically bulky salen ligands, and *cis-β*-Ru-salen carbene complexes *cis-β*-[Ru^{II}(salenL^2)(CO)(CAr_2)] (**5**; Ar = Ph: **5a**, *p*-ClC_6H_4: **5b**), electrochemical properties of **1**–**5**, and the catalytic properties of **1**–**4** towards carbene insertion into X–H (X = Si, N) bonds including detection of the corresponding Ru-carbene intermediate by ESI-MS analysis, together with stoichiometric carbene transfer reactions of **5** with a nitrosoarene. The structures of **3** and **5a** have been determined by X-ray crystallographic studies. Complex **4** catalyzed enantioselective carbene Si–H insertion with product yields up to 96% and enantioselectivities up to 84% ee. This work, to our best knowledge, provides the first examples of isolated *cis-β*-Ru-salen carbene complexes and Si–H insertion catalyzed by a Ru-salen complex.

RESULTS

Synthesis. The ligands H_2salenL^1, H_2salenL^2, and H_2salenL^4 were prepared by refluxing the corresponding diamine and salicylaldehyde in EtOH as reported in the literature, and the new ligand H_2salenL^3 was prepared by a similar procedure (see the Supporting Information). Like the preparation of bis(carbonyl) complexes (1*R*,2*R*)-**1** and *rac*-**2**,[5] reactions of $Ru_3(CO)_{12}$ with enantiopure (1*S*,2*S*)-H_2salenL^1, (*S*)-H_2salenL^2, and (*R*)-H_2salenL^4 in 1,2,4-trichlorobenzene at 185 °C under argon in the dark for 6 h afforded chiral *cis-β*-[Ru^{II}(salen)$(CO)_2$] complexes (1*S*,2*S*)-**1**, (*S*)-**2** and (*R*)-**4**, respectively (or their racemic counterparts if racemic H_2salen ligands were used; see, for example, Scheme 1). Interestingly, upon changing the H_2salen

Scheme 1. Synthesis of *cis-β* Ru-Salen Complexes 3 and 4

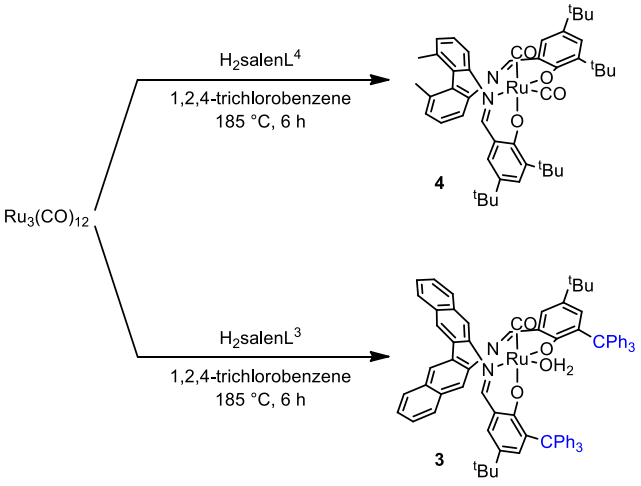

ligand to *rac*-H_2salenL[3] bearing bulky CPh_3 substituents, the reaction under the same conditions gave a mono(carbonyl) complex, *cis*-*β*-[Ru^{II}(salenL[3])(CO)(H_2O)] (*rac*-**3**, Scheme 1; the corresponding *cis*-*β*-[Ru^{II}(salenL[3])$(CO)_2$] complex was not obtained). At the end of the reactions for all these preparations, salicylaldehydes of the corresponding H_2salen ligands were detected by TLC and ^{1}H NMR, indicating partial decomposition of the H_2salen ligands under the reaction conditions.

cis-*β*-[Ru^{II}(salenL[2])(CO)(CPh_2)] (**5a**) and *cis*-*β*-[Ru^{II}(salenL[2])(CO)($C(C_6H_4$-*p*-$Cl)_2$)] (**5b**) were synthesized by irradiation of a refluxing solution of *cis*-*β*-[Ru^{II}(salenL[2])$(CO)_2$] (**2**) in MeCN with an incandescent lamp (300 W) for 3 h, to remove one of the two coordinated CO groups in **2**, followed by treatment with solutions of diazo compounds N_2CPh_2 and $N_2C(C_6H_4$-*p*-$Cl)_2$, respectively, in dichloromethane (DCM) at room temperature (Scheme 2). Slow addition of the diazo compound solutions (via a syringe pump for 30 min) was required to minimize catalytic decomposition of the diazo compounds. When the solution of **2** was directly treated with the diazo compound N_2CPh_2 or $N_2C(C_6H_4$-*p*-$Cl)_2$, without pre-irradiation with an incandescent lamp, no *cis*-*β*-Ru-salen carbene complex (**5a** or **5b**) was detected from the reaction mixture.

Scheme 2. Synthesis of *cis*-*β*-Ru-Salen Carbene Complexes 5a and 5b

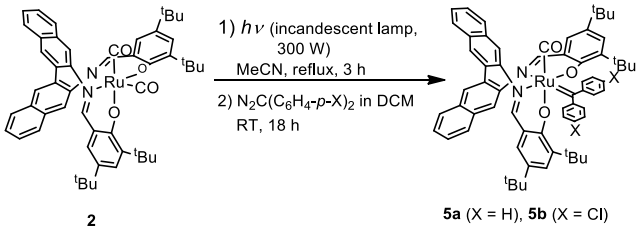

Stability and Spectroscopy. Complexes **1**, **2** and **4** are stable in the absence of light; in $CDCl_3$ solutions under dark conditions, neither isomerization nor decomposition of these complexes to mono(carbonyl) analogues, such as *cis*-*β*-[Ru^{II}(salen)(CO)(H_2O)], was observed upon standing at room temperature for at least 3 days, as revealed by ^{1}H NMR and ESI-MS analyses. Complexes **5a**,**b** are stable in open atmosphere in the solid state (for at least 1 month) in the absence of light, as revealed by UV-vis absorption spectroscopy, ^{1}H NMR and ESI-MS analyses.

In the FAB mass spectra, *cis*-*β*-[Ru^{II}(salen)$(CO)_2$] complexes **1**, **2** and **4** (in MeOH) each show three prominent signals assignable to M^+, $[M - CO]^+$ and $[M - 2CO]^+$. For *cis*-*β*-[Ru^{II}(salenL[3])(CO)(H_2O)] (**3**, in MeOH), two prominent signals assignable to $[M - H_2O]^+$ and $[M - H_2O - CO]^+$ were observed. The HR-ESI-MS analysis of **5a** revealed a signal at *m/z* 1011.4066 with the *m/z* value and isotope pattern matching that simulated for $[M + H]^+$, together with a signal at *m/z* 1033.3888 attributable to $[M + Na]^+$ (Figure 3). Similar results were obtained for the HR-ESI-MS analysis of **5b** (e.g., *m/z* 1079.3179 assignable to $[M + H]^+$).

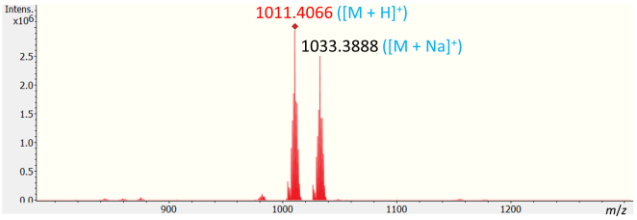

Figure 3. HR-ESI-MS spectrum of **5a** in DCM.

The ^{1}H NMR spectra of **3** and **4** in $CDCl_3$ (Figure 4), like that of **1** and **2**,[5] show well-resolved signals in diamagnetic region (0–10 ppm). The large splitting of the two H_{imine} (N=C–*H*) signals of the coordinated salenL[4] ligand in the *cis*-*β*-bis(carbonyl) complex **4** (Figure 4b), with $\Delta\delta$ = 0.53 ppm, is comparable to that reported for the salenL[1] counterpart **1** ($\Delta\delta_H$ = 0.31) and the salenL[2] counterpart **2** ($\Delta\delta_H$ = 0.57),[5] all being significantly larger than that ($\Delta\delta_H$ = 0.08 ppm) for the salenL[1] adopting a planar N_2O_2 configuration in structurally characterized *trans*-[Ru^{II}(salenL[1])(NO)(Cl)].[22]

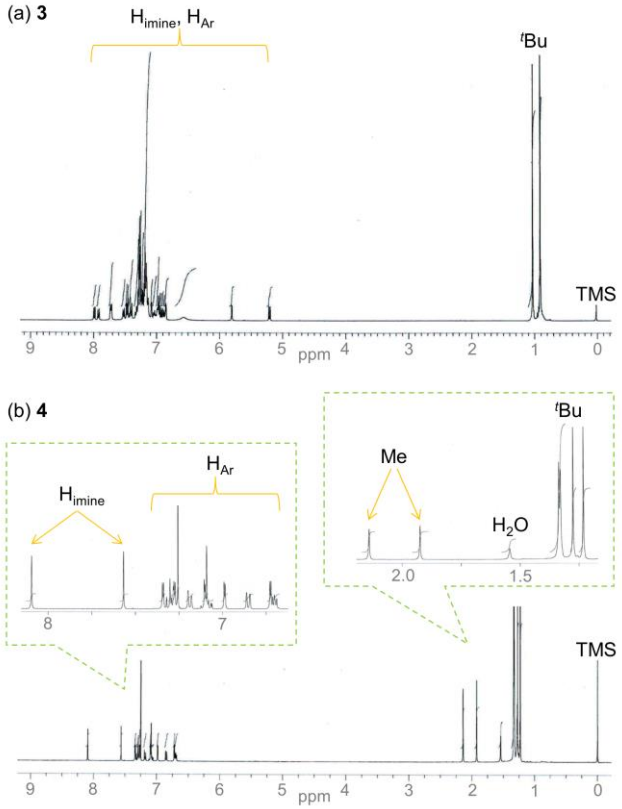

Figure 4. ^{1}H NMR spectra of (a) **3** and (b) **4** in $CDCl_3$.

The *cis*-*β*-Ru-salen carbene complexes **5a**,**b** in $CDCl_3$ also exhibit well-resolved diamagnetic ^{1}H NMR spectra (Figure S1 in the Supporting Information), like other Ru-carbene complexes such as those bearing porphyrin[18] or bis(oxazolinyl)pyridine ligands.[23] The salenL[2] ligand in **5a**,**b** gave signals analogous to, but distinct from, that in **2**,

with the most downfield H_{imine} signal appearing at δ_H 8.18 (**5a**), 8.19 (**5b**) and 8.13 (**2**) ppm. The ^{13}C NMR spectra of **5a**,**b** show a low-field signal at δ_C 337.12 and 329.95 ppm, respectively, attributable to the coordinated carbene C atom.[3,18,23]

Variable-temperature ^1H NMR spectra in $CDCl_3$ were measured using **1** and **5b** as examples (Figures S2 and S3 in Supporting Information), which revealed that the signals did not significantly change upon changing the temperature over the range of −50 to 50 °C.

The UV-vis spectral data of complexes **1–5** are presented in Table S1, and the corresponding spectra are depicted in Figure 5 for **2**, **3**, and **5a** bearing binaphthyl salen ligands and in Figures S4–S6 for **1**, **4** and **5b**. Complexes **1–4** exhibit broad absorption bands with λ_{max} between 419 and 442 nm, which could be assigned to MLCT transitions. For **4**, there is also an absorption band with λ_{max} at 366 nm (see Figure S5) attributable to intra-ligand charge transfer transitions.[24,25] In the case of **5a**,**b**, their absorption bands are similar. For example, the spectrum of **5a** (Figure 5) shows a broad band with λ_{max} at 410 nm, together with a weak low-energy shoulder absorption band at ca. 630–700 nm (log ε ~ 2.69 dm^3 mol^{-1} cm^{-1}, see Discussion section).

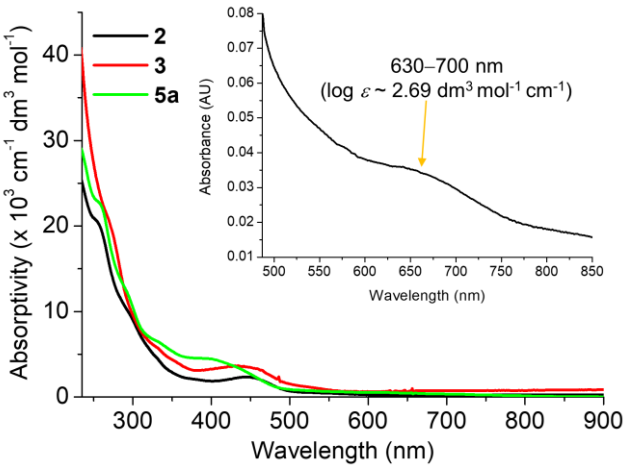

Figure 5. UV−vis absorption spectra of **2**, **3** and **5a** in DCM. Inset: a clearer view of the shoulder absorption band at 630–700 nm for **5a**.

In the IR spectra of complexes **1–5** (Figures S8–S13 and Table S2), intense bands assignable to ν(CO) were observed. The *cis*-β-bis(carbonyl) complexes **1**, **2** and **4** each exhibit two intense ν(CO) bands at ~2040 and ~1970 cm^{-1}.[26] For *cis*-β-mono(carbonyl) complex **3**, a single intense ν(CO) band at ~1940 cm^{-1} was observed (Figure S10). The *cis*-β-mono(carbene) complex **5a** or **5b**, each bearing one coordinated CO ligand, also exhibits a single intense ν(CO) band, which appears at 1977 cm^{-1} or 1976 cm^{-1}, respectively (Figures S12 and S13).

X-ray Crystal Structures. Diffraction-quality crystals of **1**·0.25MeOH and **5a**·0.5DCM were obtained by slow evaporation of their solutions in DCM/MeOH, and a diffraction-quality crystal of **3**·2DCM was grown by layering *n*-hexane on the top of a solution of **3** in DCM. The structures of the three complexes determined by X-ray crystallography (Figures 6 and 7, Figure S14) all feature a *cis*-β configuration. Selected bond distances and angles are given in Table 1.

For **1**·0.25MeOH (Figure S14), its Ru–N_{imine} and Ru–O_{OAr} distances are 2.0517(15)–2.0735(17) Å and 2.0602(13)–2.1008(14) Å respectively; the two *cis* CO ligands make a C_{CO}-Ru-C_{CO} angle of 88.26(9)°, and the Ru–C_{CO} distance for the CO ligand *trans* to the O_{OAr} atom of the salenL^1 ligand (1.858(2) Å) is shorter than that *trans* to the N_{imine} atom of the salenL^1 ligand (1.912(2) Å). These structural features are similar to those of the previously reported **1**·3MeOH.[5]

In the crystal structure of **3** (Figure 6), the Ru–N_{imine} and Ru–O_{OAr} distances fall within the ranges of 2.027(4)–2.050(4) Å and 2.071(3)–2.081(3) Å, respectively, which are comparable to those in **1** and **2**[5] (Ru–N 2.028(7)–2.090(4) Å, Ru–O 2.044(5)–2.1008(14) Å). The Ru–C_{CO} bond is *trans* to the O_{OAr} atom of the salenL^3

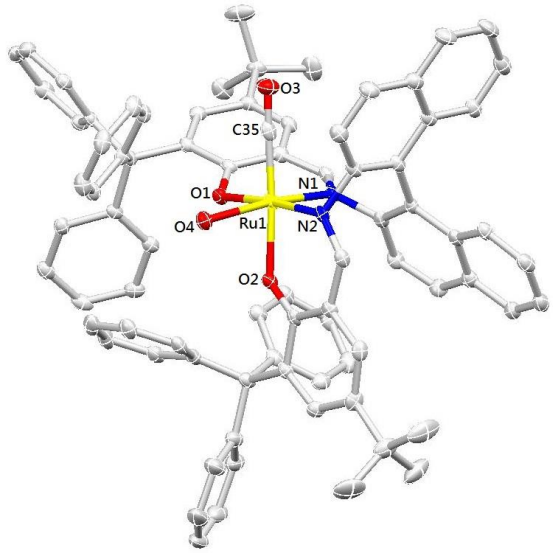

Figure 6. ORTEP diagram (50% probability) of **3**. Hydrogen atoms and solvent molecules have been omitted for clarity.

Table 1. Selected Bond Distances (Å) and Angles (Deg) of *cis*-β-Ruthenium-Salen Complexes 1, 3 and 5a

	1	3	5a
Ru–O1	2.0602(13)	2.081(3)	2.064(2)
Ru–O2	2.1008(14)	2.071(3)	2.060(2)
Ru–N1	2.0735(17)	2.027(4)	2.031(3)
Ru–N2	2.0517(15)	2.050(4)	2.202(2)
Ru–C1[a]	1.858(2)	1.842(5)	1.859(3)
Dihedral angle[b]	50.7°	74.0°	75.5°

[a]C21, C35 and C51 atoms in the ORTEP drawings of **1**, **3** and **5a**, which are generated by repeating the symmetric unit to form the whole structure, are presented as C1 atom. [b]Dihedral angle is the angle between the two phenyl planes of the salen ligand.

ligand, with a bond distance of 1.842(5) Å comparable to the Ru–C_{CO} distance of 1.837(26) Å in **2**.[5] The Ru–O_{water} bond in **3** is *trans* to a Ru–N_{imine} bond and has a distance of 2.164(3) Å, which is longer than that of the Ru–O_{OAr} bonds in the same complex. The *cis* CO and H_2O ligands in **3** make a C_{CO}-Ru-O_{water} angle of 96.75(18)°, larger than the C_{CO}-Ru-C_{CO} angles in **1** and **2** (88.26(9)°–91.4(3)°).[5] Notably, the angle formed by the two phenyl planes of the salenL[3] ligand in **3** is 74.0°, considerably larger than the corresponding angles in **1** and **2** (50.7–58.9°).[5]

Complex **5a** features a coordinated CPh_2 carbene ligand *trans* to the N_{imine} atom and a coordinated CO ligand *trans* to the O_{OAr} atom (Figure 7), corresponding to the *cis*-*β*-Ru-salen carbene species **II** depicted in the inset of Figure 2. There are two independent molecules of **5a** in the crystallographic asymmetric unit, only one of which is depicted in Figure 7. The bond angles around the $C_{carbene}$ atom (C116) are 113.7(3)° (C117–C116–C123), 119.1(2)° (C117–C116–Ru2) and 127.0(2)° (C123–C116–Ru2), which sum up to 359.8(3)° (the corresponding sum for the $C_{carbene}$ atom C52 in the other independent molecule of **5a**, not shown in Figure 7, is 359.9(3)°), indicating sp^2 hybridization of the $C_{carbene}$ atom. The Ru–$C_{carbene}$ distance of **5a** is 1.939(3) Å (Ru2–C116) and 1.967(3) Å (Ru1–C52), comparable to that of *trans*-[Ru(salen)(CAr_2)(L)] (1.910(2)–1.921(12) Å; Ar = Ph, *p*-$MeOC_6H_4$; L = MeIm, py),[3] but significantly longer than that of *trans*-[Ru(Por)(CPh_2)(L)] (e.g. 1.845(3)–1.876(3) Å; Por = porphyrin ligand TTP or F_{20}-TPP; L = MeOH, MeIm[27,28]) and *trans*-[Ru(pybox)($C(CO_2Me)_2$)Cl_2] (1.880(7) Å, pybox = bis(oxazolinyl)pyridine ligand).[23a] The two phenyl planes of the salenL[2] ligand form a considerably larger angle of 75.5° in the *cis*-*β*-Ru(CO)(CPh_2) complex **5a** than in the *cis*-*β*-Ru$(CO)_2$ complex **2** (58.9°).[5]

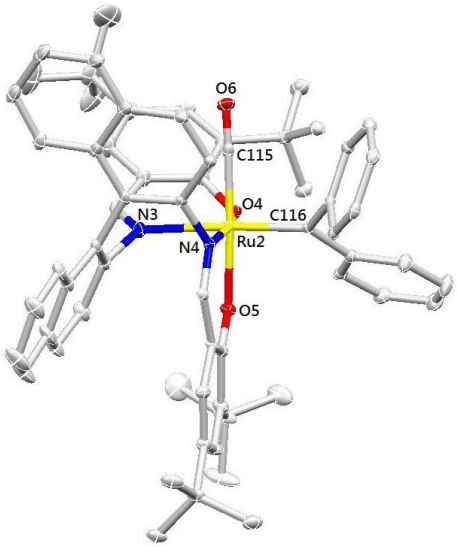

Figure 7. ORTEP diagram (50% probability) of **5a** (only one of the two independent molecules in the crystallographic asymmetric unit is shown). Hydrogen atoms and solvent molecules have been omitted for clarity.

Electrochemistry. The electrochemical properties of complexes **1**–**5** were investigated by cyclic voltammetry in DCM containing 0.1 M [^{n}Bu_4N]PF_6. The observed redox potentials (vs Ag/AgCl) are listed in Table 2, and the cyclic voltammograms are shown in Figure 8.

cis-*β*-$Ru^{II}(CO)_2$ complexes **1**, **2**, and **4**, each exhibits two oxidation waves (reversible or quasi-reversible) with $E_{1/2}$ = 0.85−0.97 V and 1.22−1.29 V. The first oxidation is likely to be associated with oxidation of Ru(II) to Ru(III). The second oxidation is attributable to ligand-centered oxidation process. This assignment is supported by the first oxidation couple of the *cis*-*β*-$Ru^{II}(CO)(H_2O)$ complex **3** with $E_{1/2}$ being less anodic than those of **1**, **2** and **4**, as replacing CO (a π-acceptor) by H_2O (a σ-donor) is expected to increase the electron density of Ru(II) and thus cathodically shift the $E_{1/2}$ of the Ru(III)/Ru(II) couple.

For *cis*-*β*-$Ru^{II}(CO)(CAr_2)$ complexes **5a**,**b**, two oxidation waves (irreversible or quasi-reversible) at E_{pa} = 0.81–0.83 V and $E_{1/2}$ = 1.16−1.19 V and a reduction wave (reversible) at $E_{1/2}$ = −1.20 to −1.29 V appear in each of their cyclic voltammograms. The oxidation waves could result from processes

Table 2. Electrochemical Data of 1–5[a]

complex	reduction (V)	oxidation (V)
1	–	0.85[b] and 1.22[b]
2	–	0.96[b] and 1.29[b]
3	–	0.59[b]
4	–	0.97[b] and 1.26[c]
5a	–1.29[b]	0.83[d] and 1.16[b]
5b	–1.20[b]	0.81[d] and 1.19[b]

[a]In CH_2Cl_2 with 0.1 M [^{n}Bu_4N]PF_6 as the electrolyte. Glassy carbon was the working electrode, Ag/AgCl was the reference electrode, and platinum wire was the counter electrode. $Cp_2Fe^{+/0}$ = 0.40 V. [b]Reversible, $E_{1/2}$. [c]Quasi-reversible, $E_{1/2}$. [d]Irreversible, E_{pa}.

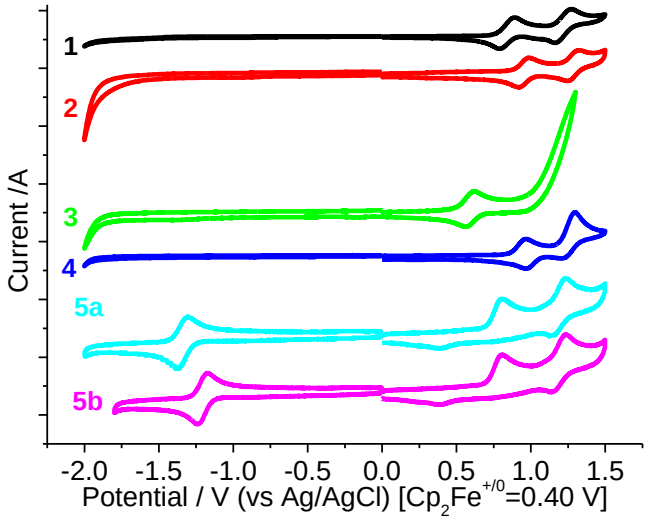

Figure 8. Cyclic voltammograms of **1**–**5** in DCM (0.1 M [^{n}Bu_4N]PF_6). Scan rate: 100 mV s^{-1}.

similar to those of **1**, **2** and **4**. The reversible reduction wave, which is absent in the cyclic voltammograms of the *cis*-β-$Ru^{II}(CO)_2$ or *cis*-β-$Ru^{II}(CO)(H_2O)$ complexes (**1**–**4**, particularly **2** bearing the same salenL^2 ligand as that in **5a**,**b**), is tentatively assigned to a carbene-based process. This assignment is consistent with the anodic shift of the reduction wave upon introducing electron-withdrawing *p*-Cl substituents on the CPh_2 carbene ligand in **5a** to give **5b** ($E_{1/2}$: from −1.29 V for **5a** to −1.20 V for **5b**).

Catalytic Carbene Si–H Insertion Reactions. At the outset, we examined the reaction of dimethylphenylsilane (**6a**) with methyl α-diazophenylacetate $N_2C(Ph)CO_2Me$ (**7a**) in 1,2-dichloroethane (DCE) at room temperature in the presence of *cis*-β-Ru-salen complexes **1**–**4** (5 mol%) under irradiation of an incandescent lamp (300 W) for 3 h. The reactions using chiral catalysts (1*S*,2*S*)-**1** and (*S*)-**2** gave product **8a** in similar yields (91%–92%) but (*S*)-**2** resulted in a higher enantioselectivity of 31% ee (Table 3, entries 1 and 2; in control experiment using catalyst (1*S*,2*S*)-**1** under dark condition, neither **8a** nor decomposition of **7a** was detected (Table 3, entry 8)). Complex *rac*-**3** exhibited markedly lower catalytic activity, affording **8a** in 65% yield (Table 3, entry 3). With use of chiral complex (*R*)-**4** as catalyst, **8a** was obtained in 96% yield with 55% ee (Table 3, entry 4). Upon changing the solvent from DCE to hexane, the reactions catalyzed by (1*S*,2*S*)-**1** and (*S*)-**2** gave **8a** in 83–84% yields with 23–36% ee (Table 3, entries 5 and 6). Notably, by using hexane as the solvent, the reaction catalyzed by (*R*)-**4** resulted in isolation of **8a** in 95% yield with 71% ee (Table 3, entry 7).

With (*R*)-**4** as catalyst and hexane as solvent, changing the diazo compound **7a** to the more bulky $N_2C(Ph)CO_2Bu^t$ (**7b**) slightly increased the enantioselectivity to 75% ee, with the corresponding product **8b** obtained in 94% isolated yield (Table 4, entry 2; the enantioselectivity slightly decreased from 75 to 73% ee upon lowering the reaction temperature from room temperature to 0 °C (Table S3)).

Table 3. Solvent and Catalyst Screening for Carbene Si–H Insertion Catalyzed by *cis*-β-Ru^{II}-Salen Complexes[a]

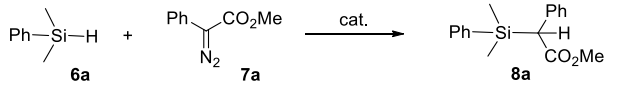

entry	cat.	solvent	yield[b] (%)	ee[c] (%)
1	(1*S*,2*S*)-**1**	DCE	92	24
2	(*S*)-**2**	DCE	91	31
3	rac-3	DCE	65	–
4	(*R*)-**4**	DCE	96	55
5	(1*S*,2*S*)-**1**	hexane	84	23
6	(*S*)-**2**	hexane	83	36
7	(*R*)-**4**	hexane	95	71
8[d]	(1*S*,2*S*)-**1**	DCE	nil[e]	–

[a]Reaction conditions: **6a** (1.5 mmol), **7a** (0.3 mmol), catalyst (5 mol%), solvent (1 mL), stirring at room temperature for 24 h under argon after irradiation with an incandescent lamp (300 W) for 3 h. [b]Isolated yield. [c]Determined by HPLC. [d]Control experiment under dark condition. [e]Product **8a** was not detected by ^{1}H NMR analysis of the crude reaction mixture.

Besides dimethylphenylsiliane (**6a**), other silanes including triethylsilane (**6b**), triphenylsilane (**6c**), tripropylsilane (**6d**), and *tert*-butyldimethylsilane (**6e**) were also used as substrates under the same reaction conditions. For the aliphatic silanes **6b**,**d**,**e**, their reactions with **7b** in hexane catalyzed by (*R*)-**4** afforded products **8c**,**e**,**f**, respectively, in yields of 84–88% and with 27–73% ee (Table 4, entries 3, 5, and 6). In the case of the bulky triarylsilane **6c**, no product **8d** was detected from the corresponding reaction (Table 4, entry 4).

The scope of diazo compounds for the (*R*)-**4**-catalyzed reaction of **6a** in hexane was examined as well, by using

Table 4. Enantioselective Carbene Si–H Insertion Catalyzed by *cis*-β-Ru^{II}-Salen Complex (*R*)-4 for Various Silanes and Diazo Compounds[a]

entry	substrate	diazo compound	product	yield[b] (%)	ee[c] (%)
1	 **6a**	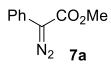 **7a**	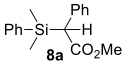 **8a**	95	71
2	 **6a**	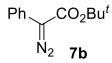 **7b**	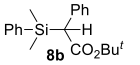 **8b**	94	75
3	 **6b**	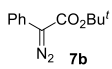 **7b**	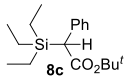 **8c**	88	73
4	 **6c**	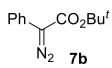 **7b**	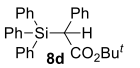 **8d**	nil[d]	-
5	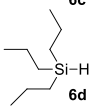 **6d**	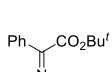 **7b**	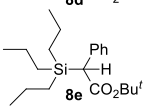 **8e**	84	27
6	 **6e**	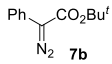 **7b**	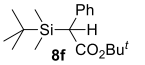 **8f**	84	38
7	 **6a**	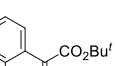 **7c**	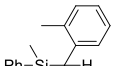 **8g**	nil[d]	-
8	 **6a**	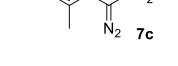 **7d**	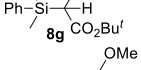 **8h**	92	73
9	 **6a**	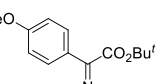 **7e**	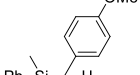 **8i**	91	84
10	 **6a**	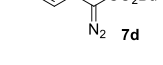 **7f**	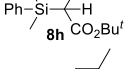 **8j**	89	60
11	 **6a**	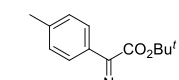 **7g**	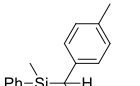 **8k**	nil[d]	-

[a]Reaction conditions: silane (1.5 mmol), diazo compound (0.3 mmol), (*R*)-**4** (5 mol%), hexane (1 mL), stirring at room temperature for 24 h under argon after irradiation with an incandescent lamp (300W) for 3 h. [b]Isolated yield. [c]Determined by HPLC. [d]Carbene Si–H insertion product was not detected by ^{1}H NMR analysis of the crude reaction mixture.

$N_2C(Ar)CO_2Bu^t$ (Ar = *o*-MeC_6H_4: **7c**, *p*-$MeOC_6H_4$: **7d**, *p*-MeC_6H_4: **7e**, *p*-ClC_6H_4: **7f**, *p*-$NO_2C_6H_4$: **7g**). For the diazo compounds **7d**,**e**,**f** bearing *p*-MeO, *p*-Me, and *p*-Cl substituents, respectively, high product yields (89–92%) and moderate-to-good enantioselectivities (60–84% ee) were obtained (Table 4, entries 8–10). The diazo compound with an *o*-Me substituent (**7c**) or with a strong electron-withdrawing *p*-NO_2 substituent (**7g**) on the phenyl group gave no detectable Si–H insertion product (Table 4, entry 7 or 11).

Catalytic Carbene N–H Insertion Reactions. The *cis*-*β*-[Ru^{II}(salen)$(CO)_2$] complexes **1**, **2** and **4** were also found to be active catalysts for carbene insertion into N–H bonds. The reactions of *tert*-butylamine with $N_2C(Ph)CO_2Me$ in DCE at 50 °C for 24 h under argon catalyzed by these complexes (after irradiation with an incandescent lamp (300W) for 3 h) afforded the carbene N–H insertion product in 72–80% yields (Table 5, entries 1–3; when (*R*)-**4** was used as the catalyst under the same conditions, the carbene N–H insertion product was obtained in 80% yield albeit without notable enantioselectivity). For the *n*-aliphatic amine substrate *n*-hexylamine, the corresponding carbene N–H insertion product was obtained in 46–55% yields under similar conditions except for a higher reaction temperature (Table 5, entries 4–6).

Table 5. Carbene N–H Insertion Reactions Catalyzed by *cis*-*β*-[Ru^{II}(salen)$(CO)_2$] Complexes[a]

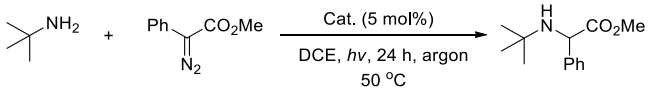

entry	cat.	conversion[b]	product (yield[b])
1	**1**	98%	78%
2	**2**	92%	72%
3	**4**	97%	80%

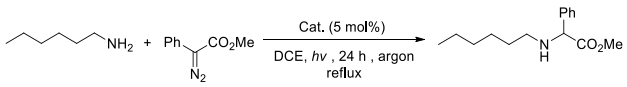

entry	cat.	conversion[b]	product (yield[b])
4	**1**	95%	52%
5	**2**	90%	46%
6	**4**	93%	55%

[a]Reaction conditions: amine (1.5 mmol), diazo compound (0.3 mmol), catalyst (5 mol%), DCE (1 mL), stirring at 50 °C (for *t*-butylamine) or at reflux (for *n*-hexylamine) for 24 h under argon after irradiation with an incandescent lamp (300W) for 3 h. [b]Determined by ^{1}H NMR using 1,1-diphenylethylene as standard.

Stoichiometric Carbene Transfer Reaction. We examined the carbene transfer reactivity of the *cis*-*β*-Ru-salen carbene complexes **5** using **5a** as example. Treatment of **5a** with excess dimethylphenylsilane (**6a**) or styrene (20 equiv) in DCE under reflux condition or light irradiation for 24 h did not give carbene transfer product (i.e. neither Si–H insertion nor styrene cyclopropanation was observed), as revealed by ^{1}H NMR analysis of the reaction mixture.

Interestingly, treatment of **5a** with excess nitrosobenzene (PhNO) at 70 °C in DCE resulted in carbene transfer to PhNO, affording the nitrone product Ph_2C=NOPh in 63% yield (Scheme 3; the nitrone product was characterized as reported in the literature[29]). After carbene transfer, **5a** was converted to the Ru(CO)(PhNO) complex *cis*-*β*-[Ru^{II}(salenL^2)(CO)(PhNO)] which was characterized by NMR and HR-ESI-MS (see the Supporting Information). We monitored the reaction between **5a** and PhNO by ^{1}H NMR spectroscopy; the resulting time course plot showed no appreciable induction period before the Ph_2C=NOPh and *cis*-*β*-[Ru^{II}(salenL^2)(CO)(PhNO)] products were formed (Figure 9).

Scheme 3. Stoichiometric Reaction between 5a and Nitrosobenzene

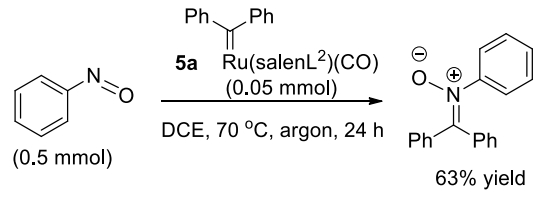

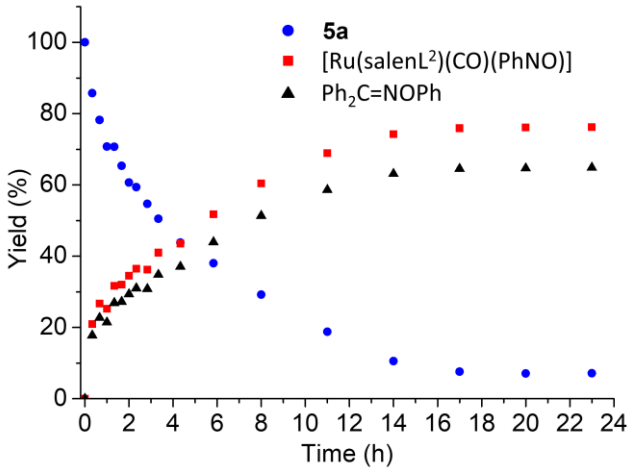

Figure 9. Time course plot of the stoichiometric reaction between **5a** and PhNO.

Detection of Reaction Intermediates in the *cis*-*β*-[Ru^{II}(salen)$(CO)_2$]-Catalyzed Carbene Si–H Insertion Reaction under Light Irradiation. The carbene Si–H insertion reactions with $N_2C(Ar)CO_2R$ catalyzed by *cis*-*β*-[Ru^{II}(salen)$(CO)_2$] complexes **1**, **2**, and **4** under irradiation of an incandescent lamp are likely to involve photolytic decarbonylation of the catalysts to form *cis*-*β*-

[Ru^{II}(salen)(CO)(solv)] followed by reaction with the diazo compound to generate Ru-carbene active intermediate *cis*-*β*-[Ru^{II}(salen)(CO)(C(Ar)CO_2R)]. Our attempts to isolate such *cis*-*β*-Ru^{II}(CO)(solv) and *cis*-*β*-Ru^{II}(CO)(C(Ar)CO_2R) intermediates have not been successful, except for the isolation of the *cis*-*β*-Ru^{II}(CO)(H_2O) complex **3** stabilized by bulky CPh_3 substituents on the salen ligand.

To help identify the reaction intermediates, HR-ESI-MS and/or UV-vis analyses of the corresponding reaction mixtures were performed using complex **2** as example. When a solution of **2** in DCE was irradiated with an incandescent lamp (300 W) under argon, a marked change of the UV-vis spectrum of this solution was observed after about 10 min (Figure S7). HR-ESI-MS measurements revealed that irradiation of a solution of **2** in refluxing MeCN with an incandescent lamp (300 W) for 15 min led to transformation of **2** to a species (*m*/*z* 885.3424, Figure 10b) assignable to the Ru(CO)(solv) complex *cis*-*β*-[Ru^{II}(salen)(CO)(MeCN)] (*m*/*z* Calcd for M^+: 885.3443), and subsequent treatment with a solution of $N_2C(Ph)CO_2Bu^t$ (4 equiv) in DCM (added via a syringe pump over 5 min, with the reaction mixture stirred for additional 10 min) generated a species exhibiting *m*/*z* 1035.4270 (Figure 10c) which is assignable to the Ru(CO)(C(Ar)CO_2R) complex *cis*-*β*-[Ru(salenL^2)(CO)(C(Ph)CO_2Bu^t)] (*m*/*z* Calcd for $[M + H]^+$: 1035.4262). Upon treatment with dimethylphenylsilane (**6a**, 50 equiv) for 15 min, the species with *m*/*z* 1035.4270 vanished, suggesting that this species is reactive with the silane substrate **6a**.

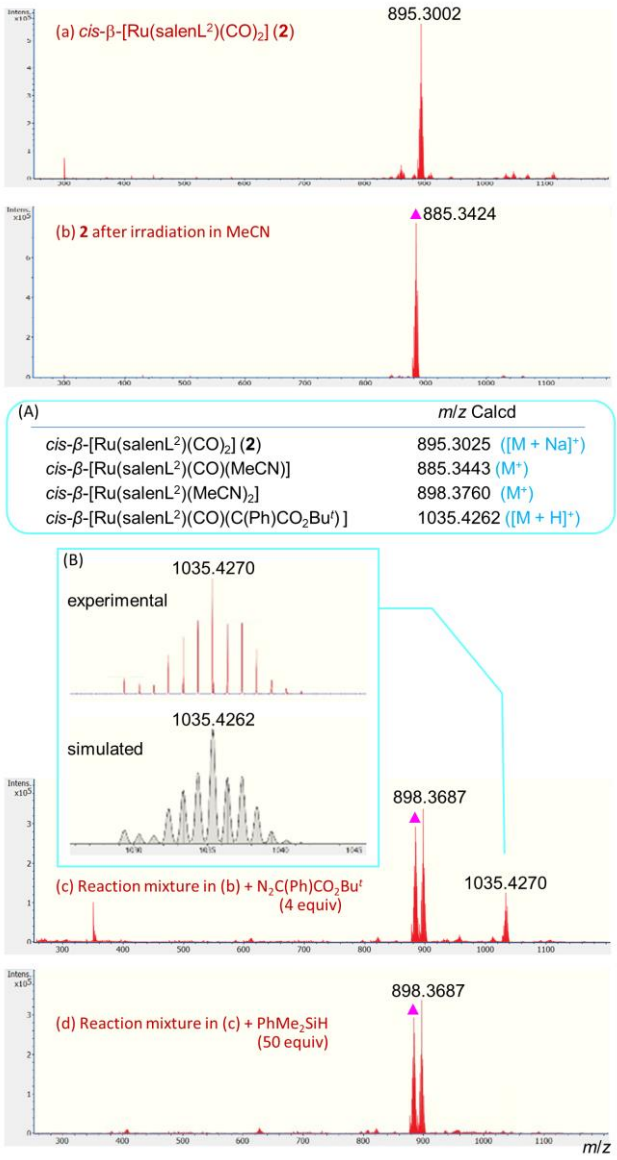

Figure 10. High-resolution ESI-MS spectra of (a) *cis*-β-[Ru(salenL^2)$(CO)_2$] (**2**), (b) **2** after irradiation with an incandescent lamp (300 W) in MeCN, (c) the reaction mixture of (b) and $N_2C(Ph)CO_2Bu^t$ (4 equiv), (d) the reaction mixture of (c) and dimethylphenylsilane (**6a**). Insets: (A) Calculated *m*/*z* values, (B) observed isotope pattern for the peak at *m*/*z* 1035.4270 and simulated isotope pattern for $\{[Ru(salenL^2)(CO)(C(Ph)CO_2Bu^t)] + H\}^+$.

DISCUSSION

cis-*β*-Bis(carbonyl) complexes *cis*-*β*-[Ru^{II}(salen)$(CO)_2$] such as **1** and **2** were previously reported as catalysts for intramolecular cyclopropanation of alkenes under light irradiation[5] via proposed *cis*-*β*-mono(carbonyl) species (formed by photolytic decarbonylation) and *cis*-*β*-Ru-salen carbene species *cis*-*β*-[Ru^{II}(salen)(CO)($CHCO_2$R)], neither of which has been isolated or clearly identified.[5] In contrast to the good stability of isolated *cis*-*β*-[Ru^{II}(salen)$(CO)_2$] complexes **1**, **2**, and **4** bearing salenL^1, salenL^2, and salenL^4 ligands, respectively, (e.g. aerobic oxidation of these complexes in $CDCl_3$ solutions is quite slow, with their yellow color gradually turning deep green over a week possibly due to the slow oxidation of Ru(II) to Ru(III)[30]), the corresponding *cis*-*β*-mono(carbonyl) counterparts for the three salen ligands, generated by photolytic decarbonylation (like dissociation of the CO ligand in $M(CO)_n$-type complexes facilitated by irradiation[31]), were found not sufficiently stable for isolation. The *cis*-*β*-Ru^{II}(CO)(H_2O) complex **3** bearing bulky salenL^3 ligand is a unique *cis*-*β*-mono(carbonyl) Ru-salen complex that has been isolated, probably owing to stabilization by the bulky CPh_3 substituents of the salenL^3 ligand. The X-ray crystal structure of **3**, featuring a H_2O ligand *trans* to the N_{imine} atom and a CO ligand *trans* to the O_{OAr} atom, is in agreement with the expected relative strength/reactivity of the two *cis* Ru–C_{CO} bonds in *cis*-*β*-[Ru^{II}(salen)$(CO)_2$] complexes, i.e., the Ru–C_{CO} bond *trans* to the imine group (a π-acceptor reducing Ru→CO π-back bonding) is weaker than that *trans* to the phenoxide group (a π-donor enhancing Ru→CO π-back bonding) and would more readily undergo ligand substitution reaction. Accordingly, the two intense *ν*(CO) bands at ~2040 and ~1970 cm^{-1} in the IR spectra of **1**, **2**, and **4** (Table S2) can be assigned to the CO ligands *trans* to the imine and phenoxide ligands, respectively, consistent with the longer Ru–C_{CO} bond *trans* to the imine group than *trans* to the phenoxide group in the X-ray crystal structures of **1** and **2**.[5]

With regard to the proposed elusive *cis*-*β*-Ru(CO)(CHCO$_2$R) or *cis*-*β*-Ru(CO)(C(Ar)CO$_2$R) species supported by salen ligands, an isolable example has yet to be obtained, though the HR-ESI-MS measurements depicted in Figure 10 provide evidence for the possible formation of *cis*-*β*-[Ru(salenL^2)(CO)(C(Ph)CO$_2$Bu^t)].

The successful isolation of stable *cis*-*β*-[Ru^{II}(salenL^2)(CO)(CAr$_2$)] complexes (**5a**,**b**) indicates a substantial stability enhancement of a *cis*-*β*-Ru-salen carbene complex upon changing the carbene group from CHCO$_2$R or C(Ar)CO$_2$R to CAr$_2$. Complexes **5a**,**b** adopting *cis*-*β*-configuration constitute a novel type of isolated Ru-carbene complexes supported by salen ligands.

The characterization of **5a**,**b** was based on HR-ESI-MS, UV-vis, and NMR measurements and, for **5a**, also by X-ray crystal structure determination and stoichiometric carbene transfer reactivity. The $C_{carbene}$ signal of **5a**,**b** at δ_C 337.12–329.95 ppm in their ^{13}C NMR spectra is comparable to, though appreciably downfield from, that reported for *trans*-[Ru(salen)(CAr$_2$)(MeIm)] complexes (δ_C 316.3–317.3 ppm; Ar = Ph, *p*-MeOC$_6$H$_4$).[3] The weak low-energy absorption at ca. 620–700 nm (log ε ~2.51–2.69 dm^3 mol^{-1} cm^{-1}) in the UV-vis spectra of **5a**,**b** was tentatively assigned to d-d transition. Such transitions have previously been reported at 520 nm (log ε 2.56 dm^3 mol^{-1} cm^{-1}) for [RuCl$_2$(CHPh)(PCy$_3$)$_2$] (Cy = cyclohexyl)[32] and at ca. 630–660 nm (log ε 2.80–3.12 dm^3 mol^{-1} cm^{-1}) for *trans*-[Ru(salen)(CPh$_2$)(L)] (L = MeIm, py).[3] In the X-ray crystal structure of *cis*-*β*-Ru(CO)(CPh$_2$) complex **5a**, the CPh$_2$ carbene ligand is *trans* to the imine group, like the H$_2$O ligand in the *cis*-*β*-Ru(CO)(H$_2$O) complex **3**; this is supportive of the formation of **5a** from a *cis*-*β*-Ru(CO)(solv) intermediate (generated by photolytic decarbonylation of the *cis*-*β*-Ru(CO)$_2$ complex **2** in solution) with its coordinated solvent molecule being replaced by the carbene group. The relatively long Ru–$C_{carbene}$ distance of **5a** (1.953(3) Å, averaged value for the two crystallographically independent molecules) is possibly associated with the presence of a *trans* imine group which competes for the π-back bonding with Ru and would weaken the pπ($C_{carbene}$)-dπ(Ru) interaction.

Considering the experimental findings obtained in this work, particularly the isolation of *cis*-*β*-Ru(CO)(CAr$_2$) complexes **5a**,**b** and HR-EI-MS detection of a species assignable to *cis*-*β*-[Ru(salenL^2)(CO)(C(Ph)CO$_2$Bu^t)], a mechanism of the chiral *cis*-*β*-[Ru^{II}(salen)(CO)$_2$]-catalyzed enantioselective carbene Si–H insertion reactions was proposed and depicted in Scheme 4, using catalyst **2** as example. This catalyst could undergo decarbonylation under light irradiation to give a *cis*-*β*-Ru^{II}(CO)(solv) species (a structural analogue of **3**). Subsequent reaction of this species with diazo compound N$_2$CR^{1}R^2 is likely to generate a *cis*-*β*-Ru(CO)(CR^{1}R^2) intermediate which is proposed to be the active species undergoing carbene transfer reactions to give the corresponding Si–H insertion products.

Scheme 4. Proposed Mechanism for *cis*-*β*-[Ru^{II}(salen)(CO)$_2$]-Catalyzed Intermolecular Carbene Insertion into Si–H Bond

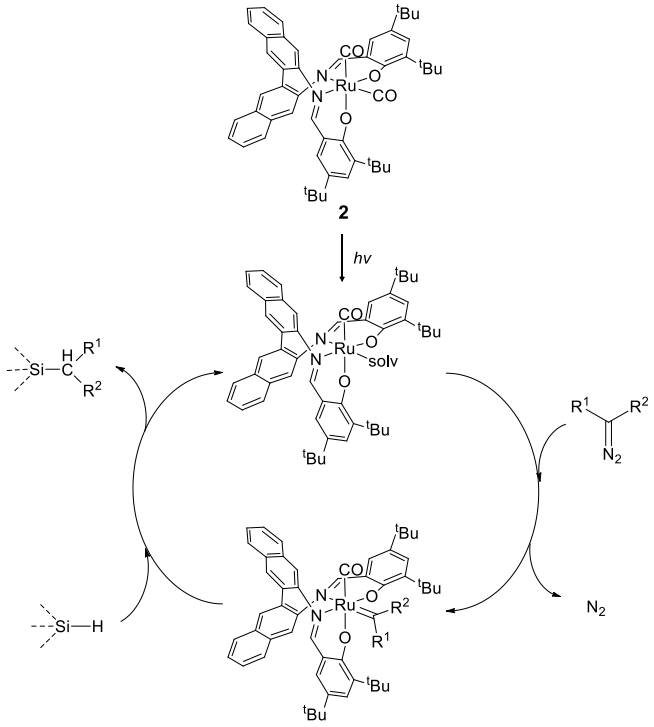

CONCLUSIONS

We have synthesized and characterized new *cis*-*β*-ruthenium–salen complexes **3**, **4**, **5a** and **5b**, including their electrochemical behavior, and also examined the catalytic properties of **1**–**4** towards carbene insertion into Si–H and/or N–H bonds.[33] Complex **3** represents a *cis*-*β*-[Ru(salen)(CO)(solv)] analogue stabilized by the binaphthyl salen ligand with bulky CPh$_3$ substituents, and complexes **5a**,**b** are unique Ru-salen carbene complexes adopting a *cis*-*β* configuration and exhibiting carbene transfer reactivity towards nitrosobenzene to give a nitrone product.[34] The chiral *cis*-*β*-[Ru^{II}(salen)(CO)$_2$] complexes (1*S*,2*S*)-**1**, (*S*)-**2**, and (*R*)-**4** can catalyze asymmetric intermolecular carbene Si–H insertion; using catalyst (*R*)-**4** which bears a biphenyl salen ligand with ^{t}Bu substituents, the reactions of an aryl silane and aliphatic silanes with aryldiazoacetates N$_2$C(Ar)CO$_2$R as the carbene sources in hexane at room temperature upon light irradiation afforded carbene Si–H insertion products in up to excellent yield and with moderate-to-good enantioselectivity. The isolation and spectroscopic/structural studies of **3** and **5a**, together with HR-ESI-MS analysis of a solution of **2** under light irradiation and its reaction mixture with N$_2$C(Ar)CO$_2$R before and

after addition of a silane substrate, provide evidence for the involvement of *cis*-*β*-ruthenium–salen mono(carbene) complexes as the key intermediates in the *cis*-*β*-[Ru^{II}(salen)$(CO)_2$]-catalyzed intermolecular Si–H insertion reactions.

ASSOCIATED CONTENT

Supporting Information

The Supporting Information is available free of charge on the ACS Publications website.

Experimental procedures, characterization of compounds, Tables S1–S6, Figures S1–S14, NMR spectra and HPLC chromatograms (PDF).

Accession Codes

CCDC 1977412, 1977413, and 1986888 contain the supplementary crystallographic data for this paper. These data can be obtained free of charge via www.ccdc.cam.ac.uk/data_request/cif, or by emailing data_request@ccdc.cam.ac.uk, or by contacting The Cambridge Crystallographic Data Centre, 12 Union Road, Cambridge CB2 1EZ, UK; fax: +44 1223 336033.

AUTHOR INFORMATION

Corresponding Author

*E-mail: cmche@hku.hk.

Author Contributions

§These authors contributed equally.

Notes

The authors declare no competing financial interest.

ACKNOWLEDGMENT

This work was supported by Hong Kong Research Grants Council (17303815 and 17301817), 13th 5-year program of Jiangsu Open University (Project No. 17SSW-Z-Q-028), and Basic Research Program-Shenzhen Fund (JCYJ20170412140251576 and JCYJ20170818141858021).

REFERENCES

(1) (a) Katsuki, T. Some Recent Advances in Metallosalen Chemistry. *Synlett* **2003**, 281–297. (b) Irie, R.; Katsuki, T. Selective aerobic oxidation of hydroxy compounds catalyzed by photoactivated ruthenium-salen complexes (selective catalytic aerobic oxidation). *Chem. Rec.* **2004**, *4*, 96-109. (c) Cozzi, P. G. Metal–Salen Schiff base complexes in catalysis: practical aspects. *Chem. Soc. Rev.* **2004**, *33*, 410–421. (d) Katsuki, T. Unique asymmetric catalysis of *cis*-β metal complexes of salen and its related Schiff-base ligands. *Chem. Soc. Rev.* **2004**, *33*, 437–444. (e) Venkataramanan, N. S.; Kuppuraj, G.; Rajagopal, S. Metal–salen complexes as efficient catalysts for the oxygenation of heteroatom containing organic compounds—synthetic and mechanistic aspects. *Coord. Chem. Rev.* **2005**, *249*, 1249–1268. (f) Baleizaõ, C.; Garcia, H. Chiral Salen Complexes: An Overview to Recoverable and Reusable Homogeneous and Heterogeneous Catalysts. *Chem. Rev.* **2006**, *106*, 3987–4043. (g) Matsumoto, K.; Saito, B.; Katsuki, T. Asymmetric catalysis of metal complexes with non-planar ONNO ligands: salen, salalen and salan. *Chem. Commun.* **2007**, 3619–3627. (h) Gupta, K. C.; Sutar, A. K. Catalytic activities of Schiff base transition metal complexes. *Coord. Chem. Rev.* **2008**, *252*, 1420-1450. (i) Shaw, S.; White, J. D. Asymmetric Catalysis Using Chiral Salen-Metal Complexes: Recent Advances. *Chem. Rev.* **2019**, *119*, 9381-9426.

(2) Munslow, I. J.; Gillespie, K. M.; Deeth, R. J.; Scott, P. Bidentate carbenoid ester coordination in ruthenium(II) Schiff-base complexes leading to excellent levels of diastereo- and enantioselectivity in catalytic alkene cyclopropanation. *Chem. Commun.* **2001**, 1638–1639.

(3) Li, G.-Y.; Zhang, J.; Chan, P. W. H.; Xu, Z.-J.; Zhu, N.; Che, C.-M. Enantioselective Intramolecular Cyclopropanation of *cis*-Alkenes by Chiral Ruthenium(II) Schiff Base Catalysts and Crystal Structures of (Schiff base)ruthenium Complexes Containing Carbene, PPh_3, and CO Ligands. *Organometallics* **2006**, *25*, 1676–1688.

(4) Fujita, H.; Uchida, T.; Irie, R.; Katsuki, T. Asymmetric Sulfimidation with *cis*-β Ru(salalen)$(CO)_2$ Complexes as Catalyst. *Chem. Lett.* **2007**, *36*, 1092–1093.

(5) Xu, Z.-J.; Fang, R.; Zhao, C.; Huang, J.-S.; Li, G.-Y.; Zhu, N.; Che, C.-M. *cis*-β-Bis(carbonyl) Ruthenium−Salen Complexes: X-ray Crystal Structures and Remarkable Catalytic Properties toward Asymmetric Intramolecular Alkene Cyclopropanation. *J. Am. Chem. Soc*. **2009**, *131*, 4405–4417.

(6) (a) Patai, S.; Rappoport, Z. Eds., *The Chemistry of organic Silicon Compounds*, John Wiley & Sons, **1989**, Part 1, Part 2. (b) Fleming, I.; Barbero, A.; Walter, D. Stereochemical Control in Organic Synthesis Using Silicon-Containing Compounds. *Chem. Rev.* **1997**, *97*, 2063–2192. (c) Brook, M. A. *Silicon in Organic, Organometallic, and Polymer Chemistry*, Willey: New York, **2000**, Chapter 12. (d) Denmark, S. E.; Beutner, G. L. Lewis Base Catalysis in Organic Synthesis. *Angew. Chem., Int. Ed.* **2008**, *47*, 1560–1638. (e) Bähr, S.; Xue, W.; Oestreich, M. C(sp^3)–Si Cross-Coupling. *ACS Catal.* **2019**, *9*, 16–24.

(7) (a) Doyle, M. P.; McKervey, M. A.; Ye, T. *Modern Catalytic Methods for Organic Synthesis with Diazo Compounds*; Wiley: New York, **1998**, p *151*. (b) Doyle, M. P.; Forbes, D. C. Recent Advances in Asymmetric Catalytic Metal Carbene Transformations. *Chem. Rev.* **1998**, *98*, 911–936.

(8) Landais, Y.; Planchenault, D. Asymmetric metal carbene insertion into the Si-H bond. *Tetrahedron Lett.* **1994**, *35*, 4565–4568.

(9) Dakin, L. A.; Schaus, S. E.; Jacobsen, E. N.; Panek, J. S. Carbenoid Insertions into the Silicon-Hydrogen Bond Catalyzed by Chiral Copper (I) Schiff Base Complexes. *Tetrahedron Lett.* **1998**, *39*, 8947–8950.

(10) Zhang, Y.-Z.; Zhu, S.-F.; Wang, L.-X.; Zhou, Q.-L. Copper-Catalyzed Highly Enantioselective Carbenoid Insertion into Si–H Bond. *Angew. Chem., Int. Ed.* **2008**, *47*, 8496–8498.

(11) (a) Buck, R. T.; Doyle, M. P.; Drysdale, M. J.; Ferris, L.; Forbes, D. C.; Haigh, D.; Moody, C. J.; Pearson, N. D.; Zhou, Q.-L. Asymmetric Rhodium Carbenoid Insertion into the Si-H Bond. *Tetrahedron Lett.* **1996**, *37*, 7631–7634. (b) Davies, H. M. L.; Hansen, T.; Rutberg, J.; Bruzinski, P. R. Rhodium(II) (*S*)-*N*-(arylsulfonyl)prolinate catalyzed asymmetric insertions of vinyl- and phenylcarbenoids into the Si-H bond. *Tetrahedron Lett.* **1997**, *38*, 1741–1744. (c) Buck, R. T.; Coe, D. M.; Drysdale, M. J.; Ferris, L.; Haigh, D.; Moody, C. J.; Pearson, N. D.; Sanghera, J. B. Asymmetric Rhodium Carbene Insertion into the Si–H Bond : Identification of New Dirhodium(II) Carboxylate Catalysts Using Parallel Synthesis Techniques. *Tetrahedron: Asymmetry* **2003**, *14*, 791–816.

(12) Chen, D.; Zhu, D.-X.; Xu, M.-H. Rhodium(I)-Catalyzed Highly Enantioselective Insertion of Carbenoid into Si–H: Efficient Access to Functional Chiral Silanes. *J. Am. Chem. Soc.* **2016**, *138*, 1498–1501.

(13) (a) Yasutomi, Y.; Suematsu, H.; Katsuki, T. Iridium(III)-Catalyzed Enantioselective Si-H Bond Insertion and Formation of an Enantioenriched Silicon Center. *J. Am. Chem.*

Soc. **2010**, *132*, 4510–4511. (b) Wang, J.-C.; Xu, Z.-J.; Guo, Z.; Deng, Q.-H.; Zhou, C.-Y.; Wan, X.-L.; Che, C.-M. Highly Enantioselective Intermolecular Carbene Insertion to C–H and Si–H Bonds Catalyzed by a Chiral Iridium(III) Complex of a D4-Symmetric Halterman Porphyrin Ligand. *Chem. Commun.* **2012**, *48*, 4299–4301. (c) Lee, C. L.; Wu, L.; Huang, J.-S.; Che, C.-M. Stable iridium(IV) complexes supported by tetradentate salen ligands. Synthesis, structures and reactivity. *Chem. Commun.* **2019**, *55*, 3606–3609.

(14) Nakagawa, Y.; Chanthamath, S.; Fujisawa, I.; Shibatomi K.; Iwasa, S. Ru(II)-Pheox-catalyzed Si–H insertion reaction: construction of enantioenriched carbon and silicon centers. *Chem. Commun.* **2017**, *53*, 3753–3756.

(15) (a) Miller, J. A.; Jin, W.; Nguyen, S. T. An efficient and highly enantio- and diastereoselective cyclopropanation of olefins catalyzed by Schiff-base ruthenium(II) complexes. *Angew. Chem., Int. Ed.* **2002**, *41*, 2953-2956. (b) Saha, B.; Uchida, T.; Katsuki, T. Asymmetric intramolecular cyclopropanation of diazo compounds with metallosalen complexes as catalyst: structural tuning of salen ligand. *Tetrahedron: Asymmetry* **2003**, *14*, 823–836. (c) Saha, B.; Uchida, T.; Katsuki, T. Highly Enantioselective Intramolecular Cyclopropanation of Alkenyl Diazo Ketones Using Ru(salen) as Catalyst. *Chem. Lett.* **2002**, 846–847. (d) Saha, B.; Uchida, T.; Katsuki, T. Intramolecular Asymmetric Cyclopropanation with (Nitroso)(salen)ruthenium(II) Complexes as Catalysts. *Synlett* **2001**, 114–116. (e) Uchida, T.; Saha, B.; Katsuki, T. Co(II)–salen-catalyzed asymmetric intramolecular cyclopropanation. *Tetrahedron Lett.* **2001**, *42*, 2521–2524.

(16) (a) Katsuki, T. Metal Complexes as Catalysts for Oxygen, Nitrogen, and Carbon-atom Transfer Reactions. *Compr. Coord. Chem. II* **2004**, *9*, 207–264. (b) Maas, G. Ruthenium-catalysed carbenoid cyclopropanation reactions with diazo compounds. *Chem. Soc. Rev.* **2004**, *33*, 183–190. (c) Lebel, H.; Marcoux, J.-F.; Molinaro, C.; Charette, A. B. Stereoselective Cyclopropanation Reactions. *Chem. Rev.* **2003**, *103*, 977–1050. (d) Davies, H. M. L.; Antoulinakis, E. G. Intermolecular Metal-Catalyzed Carbenoid Cyclopropanations. *Org. React.* **2001**, *57*, 1–326. (e) Che, C.-M.; Huang, J.-S. Ruthenium and osmium porphyrin carbene complexes: synthesis, structure, and connection to the metal-mediated cyclopropanation of alkenes. *Coord. Chem. Rev.* **2002**, *231*, 151–164. (f) Simonneaux, G.; Le Maux, P. Optically active ruthenium porphyrins: chiral recognition and asymmetric catalysis. *Coord. Chem. Rev.* **2002**, *228*, 43–60. (g) Doyle, M. P.; McKervey, M. A.; Ye, T. *Modern Catalytic Methods for Organic Synthesis with Diazo Compounds: From Cyclopropanes to Ylides*, Wiley: New York, **1998**.

(17) Park, S.-B.; Murata, K.; Matsumoto, H.; Nishiyama, H. Remote electronic control in asymmetric cyclopropanation with chiral Ru-pybox catalysts. *Tetrahedron: Asymmetry* **1995**, *6*, 2487–2494.

(18) Che, C.-M.; Huang, J.-S.; Lee, F.-W.; Li, Y.; Lai, T.-S.; Kwong, H.-L.; Teng, P.-F.; Lee, W.-S.; Lo, W.-C.; Peng, S.-M.; Zhou, Z.-Y. Asymmetric Inter- and Intramolecular Cyclopropanation of Alkenes Catalyzed by Chiral Ruthenium Porphyrins. Synthesis and Crystal Structure of a Chiral Metalloporphyrin Carbene Complex. *J. Am. Chem. Soc.* **2001**, *123*, 4119–4129.

(19) Lo, W.-C.; Che, C.-M.; Cheng, K.-F.; Mak, T. C. W. Catalytic and asymmetric cyclopropanation of styrenes catalysed by ruthenium porphyrin and porphycene complexes. *Chem. Commun.* **1997**, 1205–1206.

(20) Galardon, E.; Le Maux, P.; Simonneaux, G. Cyclopropanation of alkenes with ethyl diazoacetate catalysed by ruthenium porphyrin complexes. *Chem. Commun*. **1997**, 927–928.

(21) Frauenkron, M.; Berkessel, A. A novel chiral ruthenium porphyrin as highly efficient and selective catalyst for asymmetric cyclopropanations. *Tetrahedron Lett.* **1997**, *38*, 7175–7176.

(22) Leung, W. H.; Chan, E. Y. Y.; Chow, E. K. F.; Williams, I. D.; Peng, S. M. Metal complexes of a chiral quadridentate Schiff base. *J. Chem. Soc., Dalton Trans.* **1996**, 1229–1236.

(23) (a) Nishiyama, H.; Aoki, K.; Itoh, H.; Iwamura, T.; Sakata, N.; Kurihara, O.; Motoyama, Y. Stable Decarbonylcarbene Complexes of Bis(oxazolinyl)pyridine Ruthenium and Osmium. *Chem. Lett.* **1996**, 1071–1072. (b) Park, S.-B.; Sakata, N.; Nishiyama, H. Aryloxycarbonylcarbene Complexes of Bis(oxazolinyl)pyridineruthenium as Active Intermediates in Asymmetric Catalytic Cyclopropanations. *Chem.-Eur. J.* **1996**, *2*, 303–306.

(24) Che, C.-M.; Cheng, W.-K.; Mak, T. C. W. Synthesis and reactivities of trans-dioxoosmium(VI) Schiff-base complexes. X-ray crystal structure of dioxo[*N*,*N*'-(1,1,2,2-tetramethylethylene)bis(3-*tert*-butylsalicylideneaminato)]osmium(VI). *Inorg. Chem.* **1988**, *27*, 250–253.

(25) Miskowski, V. M.; Gray, H. B.; Hopkins, M. D. *Adv. Transition Met. Coord. Chem.* **1996**, *1*, 159 and references therein.

(26) The ν(CO) bands of **1**, **2**, and **4** are significantly different from those (1890 and 1920 cm^{-1}) of the *cis*-$[Ru^{II}(salenL^1)(CO)_2]$ prepared from the reaction of $Na_2salenL^1$ with $[\{Ru(CO)_2Cl_2\}_n]$ in THF.[22]

(27) Kawai, M.; Yuge, H.; Miyamoto, T. K. A ruthenium(II)–porphyrin–carbene complex with a weakly bonded methanol ligand. *Acta Crystallogr., Sect. C* **2002**, *58*, M581–M582.

(28) Li, Y.; Huang, J.-S.; Xu, G.-B.; Zhu, N.; Zhou, Z.-Y.; Che, C.-M.; Wong, K.-Y. Spectral, Structural, and Electrochemical Properties of Ruthenium Porphyrin Diaryl and Aryl(alkoxycarbonyl) Carbene Complexes: Influence of Carbene Substituents, Porphyrin Substituents, and *trans*-Axial Ligands. *Chem.-Eur. J.* **2004**, *10*, 3486–3502.

(29) Rodrigo, E.; Alonso, I.; Cid, M. B. A Protocol To Transform Sulfones into Nitrones and Aldehydes. *Org. Lett.* **2018**, *20*, 5789–5793.

(30) (a) Murray, K. S.; Van, d. B. A.; West, B. O. Ruthenium complexes with a tetradentate salicylaldimine Schiff base. *Aust. J. Chem.* **1978**, *31*, 203–207. (b) Man, W.-L.; Kwong, H.-K.; Lam, W. W. Y.; Xiang, J.; Wong, T.-W.; Lam, W.-H.; Wong, W.-T.; Peng, S.-M.; Lau, T.-C. General Synthesis of (Salen)ruthenium(III) Complexes via N···N Coupling of (Salen)ruthenium(VI) Nitrides. *Inorg. Chem.* **2008**, *47*, 5936–5944.

(31) (a) Lian, T.; Bromberg, S. E.; Asplund, M. C.; Yang, H.; Harris, C. B. Femtosecond Infrared Studies of the Dissociation and Dynamics of Transition Metal Carbonyls in Solution. *J. Phys. Chem.* **1996**, *100*, 11994–12001. (b) Joly, A. G.; Nelson, K. A. Femtosecond transient absorption spectroscopy of chromium hexacarbonyl in methanol: observation of initial excited states and carbon monoxide dissociation. *J. Phys. Chem.* **1989**, *93*, 2876–2878. (c) Joly, A. G.; Nelson, K. A. Metal carbonyl photochemistry in organic solvents: Femtosecond transient absorption and preliminary resonance Raman spectroscopy. *Chem. Phys.* **1991**, *152*, 69–82. (d) Gabrielsson, A.; Za, S. Ultrafast Photochemical Dissociation of an Equatorial CO Ligand from Trans (X,X)-$[Ru(X)_2(CO)_2(Bpy)]$(X = Cl, Br, I): A Picosecond Time-Resolved Infrared Spectroscopic and DFT Computational Study. *Inorg. Chem.* **2004**, *43*, 7380–

7388. (e) Gabrielsson, A.; Towrie, M.; Záliš, S.; Vlček, A. Nanosecond CO Photodissociation and Excited-State Character of [Ru(X)(X′)(CO)$_2$(*N*,*N*′-Diisopropyl-1,4-Diazabutadiene)] (X = X′ = Cl or I; X = Me, X′ = I; X = $SnPh_3$, X′ = Cl) Studied by Time-Resolved Infrared Spectroscopy and DFT Calculations. *Inorg. Chem.* **2008**, *47*, 4236–4242. (f) Mansour, A. M. Rapid Green and Blue Light-Induced CO Release from Bromazepam Mn(I) and Ru(II) Carbonyls: Synthesis, Density Functional Theory and Biological Activity Evaluation. *Appl. Organomet. Chem.* **2017**, *31*, e3564.

(32) Wong, C.-Y.; Che, C.-M.; Chan, M. C. W.; Leung, K.-H.; Phillips, D. L.; Zhu, N. Probing the Ruthenium−Cumulene Bonding Interaction: Synthesis and Spectroscopic Studies of Vinylidene− and Allenylidene−Ruthenium Complexes Supported by Tetradentate Macrocyclic Tertiary Amine and Comparisons with Diphosphine Analogues of Ruthenium and Osmium. *J. Am. Chem. Soc.* **2004**, *126*, 2501–2514.

(33) We are aware of no other metal-salen complexes that have been used as catalysts for carbene N–H insertion reactions, despite previous reports on such reactions catalyzed by the complexes of several transition metals including Ru. For recent reviews on or involving metal-catalyzed carbene insertion into Si–H or N–H bonds, see: (a) Zhu, S.-F.; Zhou, Q.-L. Transition-Metal-Catalyzed Enantioselective Heteroatom-Hydrogen Bond Insertion Reactions. *Acc. Chem. Res.* **2012**, *45*, 1365-1377. (b) Gillingham, D.; Fei, N. Catalytic X–H insertion reactions based on carbenoids. *Chem. Soc. Rev.* **2013**, *42*, 4918-4931. (c) Burtoloso, A. C. B.; Santiago, J. V.; Bernardim, B.; Talero, A. G. Advances in the Enantioselective Metalcatalyzed N–H and O–H Insertion Reactions with Diazocar-bonyl Compounds. *Curr. Org. Synth.* **2015**, *12*, 650-659. (d) Keipour, H.; Carreras, V.; Ollevier, T. Recent progress in the catalytic carbene insertion reactions into the silicon-hydrogen bond. *Org. Biomol. Chem.* **2017**, *15*, 5441-5456.

(34) For an example of metal-mediated quinoid carbene transfer to nitrosoarenes to afford nitrones, see: Wang, H.-X.; Wan, Q.; Wu, K.; Low, K.-H.; Yang, C.; Zhou, C.-Y.; Huang, J.-S.; Che, C.-M. Ruthenium(II) Porphyrin Quinoid Carbene Complexes: Synthesis, Crystal Structure, and Reactivity toward Carbene Transfer and Hydrogen Atom Transfer Reactions. *J. Am. Chem. Soc.* **2019**, *141*, 9027-9046.

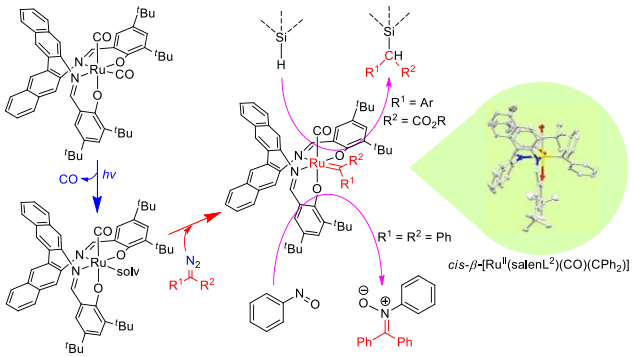
CO
hv
solv
N2
R1 = Ar
R2 = CO2R
R1 = R2 = Ph
cis-β-[RuII(salenL2)(CO)(CPh2)]